Research article

Protective effects of the bioactive peptide from maggots against skin flap ischemia–reperfusion injury in rats

Hao Chen [a],[1], Tianqi Zhang [a],[1], Su Yan [a], Shan Zhang [a], Qiuyue Fu [a], Chuchu Xiong [a], Lina Zhou [c], Xiao Ma [d], Rong Wang [b],[*], Gang Chen [a],[**]

[a] Department of Plastic Surgery, Jiangsu Province Hospital of Traditional Chinese Medicine, Nanjing, Jiangsu, PR China
[b] College of Life Science, Nanjing Normal University, Nanjing, Jiangsu, PR China
[c] Zhangjiagang Hospital of Traditional Chinese Medicine Affiliated to Nanjing University of Chinese Medicine, Zhangjiagang, Jiangsu, PR China
[d] Yixing Hospital of Traditional Chinese Medicine Affiliated to Nanjing University of Chinese Medicine, Yixing, Jiangsu, PR China

A R T I C L E I N F O

A B S T R A C T

Ischemia–reperfusion (I/R) injury is a frequently observed complication after flap surgery, and it affects skin flap survival and patient prognosis. Currently, there are no proven safe and effective treatment options to treat skin flap I/R injury. Herein, the potential efficacies of the bioactive peptide from maggots (BPM), as well as its underlying mechanisms, were explored in a rat model of skin flap I/R injury and LPS- or H_2O_2-elicited RAW 264.7 cells. We demonstrated that BPM significantly ameliorated the area of flap survival, and histological changes in skin tissue *in vivo*. Furthermore, BPM could markedly restore or enhance Nrf2 and HO-1 levels, and suppress the expression of pro-inflammatory cytokines, including TLR4, p-IκB, NFκB p65, p-p65, IL-6, and TNF-α in I/R-injured skin flaps. In addition, BPM treatment exhibited excellent biocompatibility with an adequate safety profile, while it exhibited superior ROS-scavenging ability and the upregulation of antioxidant enzymes *in vitro*. Mechanistically, the above benefits related to BPM involved the activation of Nrf2/HO-1 and suppression of TLR4/NF-κB pathway. Taken together, this study may provide a scientific basis for the potential therapeutic effect of BPM in the prevention of skin flap I/R injury and other related diseases.

1. Introduction

Flap transplantation is a critical technological approach in plastic and reconstructive surgery [1,2]. However, flap necrosis can be a catastrophic problem after reconstructive flap surgery, despite its low incidence. Ischemia–reperfusion (I/R) injury has been identified as the major factor that induces surgical skin flap or even organ dysfunction [3]. Currently, I/R injury may occur during the abrupt restoration of circulation after long-term ischemia, and its associated mechanisms can be quite complicated. Multiple factors, such as high levels of proinflammatory cytokine accumulation, excess reactive oxygen species (ROS) production during reperfusion, and epithelial apoptosis induction, have important implications for the pathogenic mechanisms of different I/R injury types during tissue injury or organ dysfunction [4–6]. The level of malondialdehyde (MDA) is served as a reliable biomarker of lipid peroxidation (LPO),

which is activated in I/R injury [7,8]. Enzymes are affected from ROS and LPO production, so superoxide dismutase (SOD) and catalase (CAT) are antioxidant enzymes that play an essential role against oxidative stress [9]. Therefore, antioxidants could protect cells against damage in flap transplantation and other related diseases [10,11]. The TLR4/NF-κB and Nrf2 pathways are suggested to be related to intracellular signaling during I/R injury [12,13].

Currently, to improve flap survival surgical technology, operation time, and medication therapy are being improved [3]. However, it should be noted that the aforementioned approaches may not be universally applicable due to the uncontrollable and heterogeneous nature of individuals [3]. Many strategies aimed at preventing skin flap failure have been proposed. For example, hyperbaric oxygen preconditioning and ischemic preconditioning were demonstrated to provide a promising clinical result [14,15]. However, the long-term effect and safety of clinical preconditioning still require further investigation. Many pharmacological therapies (e.g., melatonin, aprotinin, and heparin) have also been shown to improve flap tolerance [16–18], but few drugs are currently available for clinical application. To improve medication effectiveness and ameliorate associated systemic adverse reactions, the discovery of new specific medications is important.

Insects represent a great and unexplored source of beneficial compounds that can be used in medical treatment [19]. Maggots, also called "*WuGuChong*" in traditional Chinese medicine, represent *Lucilia sericata* larvae. They are critical medical insects that have efficient immune defense mechanisms. Additionally, they contain abundant amino acids, proteins, dietary fibers, vitamins and unsaturated fatty acids [20,21]. Housefly maggots have been used in clinical practice for treating patients with wounds, ecthyma, or bacterial infections in digestive organs [22–24]. Maggot treatment, which is the most rapid and most efficient debridement treatment for wounds involving infections and tissue necrosis, has favorable antimicrobial effects [25]. Recently, maggot extracts have been demonstrated to have antibacterial and anti-inflammatory effects, promote wound healing, and inhibit the progression of diabetes and atherosclerosis [26,27].

Over the past 10 years, many bioactive peptides from insects have been discovered *in vitro* [28,29]. Hall et al. [30] identified antihypertensive, antiglycemic, and anti-inflammatory peptides derived from the gastrointestinal digests of cricket (*Gryllodes sigillatus*). Probably the best known is the carmine dye obtained from the cochineal (*Dactylopius coccus*), which is widely used as a natural colorant in cosmetics, foods, pharmaceuticals, textiles, and plastics [31]. In addition to providing essential amino acids and energy, they also exert various biological effects, including antioxidative, anti-inflammatory and immunomodulatory effects [32,33]. Nonetheless, prior works regarding bioactive compounds in maggots have focused mostly on polysaccharides [27,34], and no existing study has analyzed the antioxidative and anti-inflammatory activities of the bioactive peptide from maggots (BPM).

Consequently, the aim of our study was to investigate the therapeutic effects of BPM on skin flap of rat followed by I/R injury and whether the TLR4/NF-κB and Nrf2/HO-1 pathways were involved in. Our study demonstrated that BPM was promising in the prevention of I/R injury in the transplantation of skin flap.

2. Materials and methods

2.1. Preparation of the BPM

The amino acid composition and sequence of the BPM (Gly-Tyr-Gly-Gly-Tyr-Gly-Gly-Phe-Gly-Arg) were provided by the State Key Laboratory of Analytical Chemistry for Life Science & Jiangsu Key Laboratory of Molecular Medicine, Medical School, Nanjing University. The product purity was >99 %, as detected by HPLC (Fig. S1). BPM was dissolved in normal saline to be used in subsequent experiments.

2.2. Flap I/R model establishment

A total of 30 male Sprague–Dawley rats (8–10 weeks old, 250–300 g) were acquired at the Model Animal Research Center of Nanjing University (China) and kept under specific pathogen-free (SPF) conditions at 25 °C, 50 % relative humidity and a 12-h/12-h light/dark cycle. The animals were permitted to eat food and drink water preoperatively and postoperatively. Rats were subsequently randomized into three groups (n = 10 for each group): the sham (sham), I/R injury (I/R), or I/R injury with BPM treatment (I/R + BPM) groups. The rats in the I/R + BPM group were orally administered BPM (20 mg/kg) once a day for 1-week preoperatively, while other groups were given normal saline as control.

After the rats were weighed, they were intraperitoneally injected with sodium pentobarbital solution (40 mg/kg). Following eyelash reflex detection, each rat was placed on a constant-temperature bench and fixed in place. After the hair was removed, the skin was disinfected with iodophor alcohol applied t on the right side of the back. Thereafter, one cross-regional flap of 9 cm × 2 cm was cut, where the iliolumbar artery (area I) was used as the pedicle, while the valve area spanned from the posterior intercostal artery to the thoracic dorsal artery (both of which were ligated) (area II). Following complete skin flap lifting, hemostasis was achieved, and sutures were used to close the skin 0.5 cm from the skin edge at 1 cm intervals [35]. The vascular bundle of the rats in I/R group was clamped with a microvascular clamp for 3 h to induce skin flap ischemia, while the rats in the sham group were not clamped [36].

All animal experiments complied with the ARRIVE guidelines and were carried out in accordance with either the U.K. Animals (Scientific Procedures) Act, 1986 and associated guidelines, the European Communities Council Directive 2010/63/EU or the National Institutes of Health – Office of Laboratory Animal Welfare policies and laws. This study was approved by the Ethics Committee of Nanjing Normal University, with ethics approval reference 2023-05-615A. All the experiments were carried out in accordance with the guidelines of the China Council on Animal Care and Use. Inhumane behaviors were not applied to the rats unless necessary.

2.3. Skin flap survival evaluation

Rats were sacrificed at 8 days postsurgery, and a digital camera was used to take photographs of the flaps. The flap necrotic area was measured with the use of the Image-Pro Plus V6.0 image analysis system, and the following formula was used to calculate the flap survival rate: flap survival rate = flap survival area (cm^2)/total flap area (cm^2) × 100 %. The necrosis of skin flaps was determined based on black color, tissue retraction, hard texture, low elasticity, and nonbleeding when the flap was cut [35]. After taking photographs, the middle of the flap tissue (1 × 1 cm^2 in size) from the proximal area of the vascular axis of the skin flap was collected, and diced into small blocks for further study. Blood samples were collected from the eye socket of mice. Samples for biochemical experiments were stored at −20 °C.

2.4. Histological examination of the skin flap

The flap tissue samples were fixed with 4 % paraformaldehyde, embedded in paraffin, and cut into 4-μm sections. Sections were deparaffinized and subjected to deparaffinization and hematoxylin & eosin (HE) staining. The tissue damage score was subsequently calculated to assess histological changes in HE-stained slides according to previous methods [36,37] after mild modifications. Specifically, the tissue damage score was determined based on pathological results, such as intravascular microthrombosis, hyperemia and inflammatory cell infiltration, as follows: 0 (none), 1 (trivial), 2 (mild), 3 (moderate), and 4 (severe). Finally, the flap tissue structure and cells were monitored [36].

2.5. Oxidative stress status and inflammatory factors evaluation

This work evaluated flap oxidative stress status by determining the levels of malondialdehyde (MDA), superoxide dismutase (SOD), glutathione peroxidase (GSH-Px), and myeloperoxidase (MPO) within skin flap tissue. In brief, 1 × 1 cm^2 of tissue was isolated from the flap center of each group, after which the samples were weighed, homogenized and diluted with ddH$_2$O$_2$ to 10 % (v/v) within an ice bath. After 15 min of centrifugation of the homogenate at 600×g and 4 °C, the supernatants were harvested to measure MDA, SOD, GSH-Px, and MPO levels using a commercial kit in accordance with the manufacturer's instructions (Nanjing Jiancheng Bioengineering Institute, Nanjing, China). The concentrations of TNF-α and IL-6 were measured by ELISA kits according to the manufacturer's instructions (Elabscience Biotechnology, Wuhan, Hubei, China).

2.6. Skin flap mRNA extraction and RT−qPCR

Total RNA was isolated from the skin flaps of the rats with RNA Miniprep reagent (Beyotime, China) in accordance with specific protocols and was subsequently reverse transcribed into cDNA (Vazyme Biotech, Nanjing, China). *TLR4*, *TNF-α*, *IL-6*, *IL-1β*, *Nrf2* and *HO-1* levels were determined using SYBR Green PCR Master Mix (Vazyme Biotech, Nanjing, China). Additionally, an ABI Viia 7 Real-Time PCR system (ABI USA, Los Angeles, CA, USA) was used for RT−qPCR, with GAPDH serving as the endogenous reference. Table 1 lists all the primers used. The $2^{-\Delta\Delta Ct}$ approach was utilized for calculating relative mRNA expression.

2.7. Western blot analysis

Total protein samples from the skin flaps were separated via 10 % SDS−PAGE and subsequently transferred to PVDF membranes (Millipore, Boston, MA, USA). Thereafter, 5 % bovine serum albumin in combination with TBST was added to the membranes, which were incubated overnight at 4 °C with primary antibodies against TLR4, *p*-IκB, NFκB p65, p-p65, IL-6, Keap1, TNF-α, Nrf2, HO-1 and GAPDH (1:2000; Abcam, USA). Thereafter, goat anti-rabbit secondary antibody (1:40,000) was added for further membrane incubation. Then, the membranes were rinsed three times, and the bands were visualized with a chemiluminescent agent (Vazyme Biotech, Nanjing, China). Finally, ImageJ software was used for image analysis. All protein bands were normalized to the band corresponding to GAPDH.

2.8. Cell culture

RAW 264.7 murine macrophages were obtained from the Chinese Academy of Sciences cell bank and cultivated in DMEM (Gibco,

Table 1
Primer sequences used in RT−qPCR.

Gene	Forward	Reverse
TLR4	TCTGCCCTGCCACCATTTACA	CAGGTCT-AAAGAGAGATTGAC
TNF-α	CCAACAAGGAGGAGAAGTTCC	CTCTGCTTGGTGGTTTGCTAC
IL-6	ACAAAGCCAGAGTCCTTCAGAG	GGCAGAGGGGTTGACTT
IL-1β	GGAACCCGTGTCTTCCTAAAG	CTGACTTGGCAGAGGACAAAG
Nrf2	AACAACGCCCTAAAGCA	TGGATTCACATAGGAGC
HO-1	CACGTATACCCGCTACCT	CCAGTTTCATTCGAGCA
GAPDH	CGCTTCACGAATTTGCGTGTCAT	GAAGATGGTGATGGGATTTC

USA) supplemented with 10 % fetal bovine serum (Gibco, USA) and 1 % penicillin/streptomycin (Gibco, USA) under 5 % CO_2 and 37 °C conditions. The passage of Raw 264.7 cells was conducted every other day to prevent autodifferentiation. A Scepter™ 2.0 Cell Counter (Millipore, USA) was used to maintain a 50–80 % cell density. Only cells at the exponential phase were used in subsequent analyses.

2.9. Cell viability detection through the CCK-8 assay

RAW 264.7 cells ((1 × 10^4/well) were inoculated into a 96-well microplate for a 24-h period under 5 % CO_2 and 37 °C conditions. Thereafter, the cells were subjected to treatment with sterilized BPM filtered with a 0.22 μm filter membrane at various doses (50, 100, 200, 400, and 800 μg/mL) for a 24-h period, and cell viability was measured using a Cell Counting Kit-8 (CCK-8; Vazyme, China). After incubation for 24 h, CCK-8 solution was added to each well, after which the cells were incubated at 37 °C. The absorbance was measured with a microplate reader at 450 nm (A450). Every assay was conducted in triplicate to obtain the average value.

2.10. In vitro evaluation of the anti-inflammatory and antioxidant activities of BPM

To further investigate whether BPM exerts anti-inflammatory and antioxidative effects on cells, inflammation was aggravated by the addition of lipopolysaccharide (LPS) [38]. Thereafter, we inoculated RAW 264.7 cells into 6-well plates (5 × 10^5 cells/ml) and introduced sterilized BPM (50, 100, 200 μg/mL) filtered with a 0.22 μm filter membrane into RAW 264.7 cell medium and incubated the mixture for 40 min at 37 °C. Furthermore, LPS (1 μg/ml) was introduced to induce inflammatory responses by further incubation for 8 h. Then, we detected inflammatory markers and oxidative stress markers by Western blot analysis (TLR4, IL-6, TNF-α, p-IκB, p-p65, Nrf2, HO-1, and Keap1).

On the other hand, the ROS-fluorescent probe (Thermo Fisher) was added for 30 min of RAW 264.7 cell incubation, followed by the addition of sterilized BPM (200 μg/mL) to DMEM. After coincubation for 30 min, H_2O_2 (100 μM) was added to induce ROS generation for a 30-min period [38]. Cells incubated with only the ROS-fluorescent probe were set as the control group, while those treated with both the probe and H_2O_2 were set up as the H_2O_2 group. The fluorescence intensity was determined via BD flow cytometry. Then, fluorescence microscopy was conducted for image acquisition at an excitation wavelength of 480 nm (the emission wavelength = 525 nm). The levels of SOD and GSH-Px were measured by commercial kits according to the manufacturer's instructions (Nanjing Jiancheng Bioengineering Institute, Nanjing, China). To examine the abilities of BPM in scavenging free radicals, we evaluated them using DPPH according to the method as described previously [39].
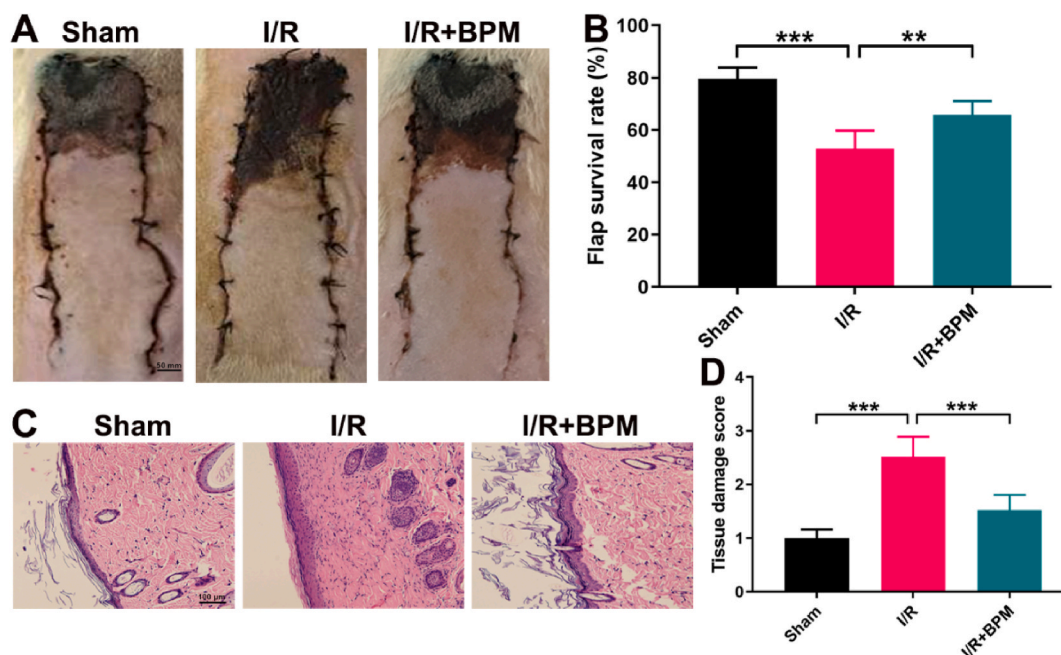

Fig. 1. The bioactive peptide from maggots (BPM) mitigated Ischemia−reperfusion (I/R) injury within skin flaps sutured to rats. (A) Representative images of the skin flaps in each group (scale bar: 50 mm). (B) Flap survival rate after I/R injury. (C) Typical H&E staining images showing tissue damage in each group and microthrombi in skin flaps treated with BPM (scale bar: 100 μm). The I/R group exhibited severe hyperemia, inflammatory cell infiltration, and intravascular microthrombi. (D) Tissue damage score of each group. The score of the BPM treatment group was markedly lower than that of the I/R group. The results are presented as the means ± SDs. *P < 0.05, **P < 0.01, and ***P < 0.001; ns, not significant.

2.11. Statistical analysis

GraphPad Prism 9.00 (GraphPad Software, Inc., La Jolla, CA, USA) was used for statistical analysis. Two-tailed Student's t tests were used to compare the significance of differences between two groups. $p < 0.05$ indicated statistical significance. The results were obtained from three or more separate assays.

3. Results

3.1. BPM alleviated skin flap I/R injury

To observe the beneficial effect of BPM on skin flap survival after I/R injury, skin morphological changes and flap survival rates were analyzed. In general, the necrotic tissue in the flap was gray, brown or black, with no elasticity. In contrast, the surviving flap was white or pink and maintained normal elasticity (Fig. 1A). The average flap survival rates of the Sham, I/R, and I/R + BPM groups at 8 days post-operation were 79.3 ± 3.5 %, 42.1 ± 4.0 %, and 62.6 ± 5.1 %, respectively. Clearly, the I/R group exhibited a markedly decreased flap survival rate in comparison with that of the Sham group. In contrast, compared with those in the I/R group, the flap survival rate in the I/R + BPM group was significantly higher, indicating markedly improved tissue injury (Fig. 1B).

Additionally, histopathological changes in the skin flap after I/R injury were monitored. The stratum corneum and flap subcutaneous tissue did not exhibit any abnormalities or significant edema in the Sham group (Fig. 1C). The scattered distribution of a low proportion of neutrophils within the interstitial space was observed, with near arrangement of fibers and an intact blood vascular wall in the Sham group. Nonetheless, edema and exfoliation were observed in a portion of the epidermis in the I/R group (Fig. 1C). Fracture and disordered arrangement of the fiber structure were also observed. Inflammatory cell infiltration was observed within the flap. In contrast, overall, the flap tissue structure was intact, with mild edema and inflammatory cell infiltration in the BPM treatment group (Fig. 1C). Neat fiber structure could be seen, the blood vascular wall was intact, and the tissue damage score was significantly decreased compared to I/R group (Fig. 1D). We also examined H&E–stained sections of crucial metabolic organs, such as the hearts, livers, spleens, kidneys, and lungs. No structural differences or signs of inflammatory cell infiltration were found (Fig. S2A). Furthermore, we analyzed serum biochemical markers of hepatic and renal functions, namely, alanine aminotransferase (ALT), aspartate aminotransferase (AST), blood urea nitrogen (BUN), and creatinine (Cr), and found no indications of damage (Fig. S2B).

3.2. BPM inhibited oxidative stress and inflammation during skin flap I/R injury

I/R injury typically results in the generation of excessive inflammatory factors, such as TNF-α and IL-1β, as well as IL-6. In addition, MDA, SOD, MPO, and GSH-Px are key oxidative stress markers during I/R injury. To assess oxidative stress injury resulting from skin flap I/R injury, MDA, MPO, GSH-Px, and SOD levels were analyzed within surgical flaps. The downregulation of SOD and GSH-Px after I/R injury could be reversed by BPM treatment (Fig. 2A and B). The I/R group presented higher levels of MDA and MPO than did the Sham group, while BPM treatment markedly downregulated the above markers of oxidative stress (Fig. 2C and D). Moreover, BPM treatment inhibited the expression of proinflammatory factors. As a result, TNF-α and IL-6 expression markedly decreased in the BPM treatment groups compared to that in the I/R injury groups (Fig. 2E and F). Based on the above findings, BPM mitigated oxidative stress
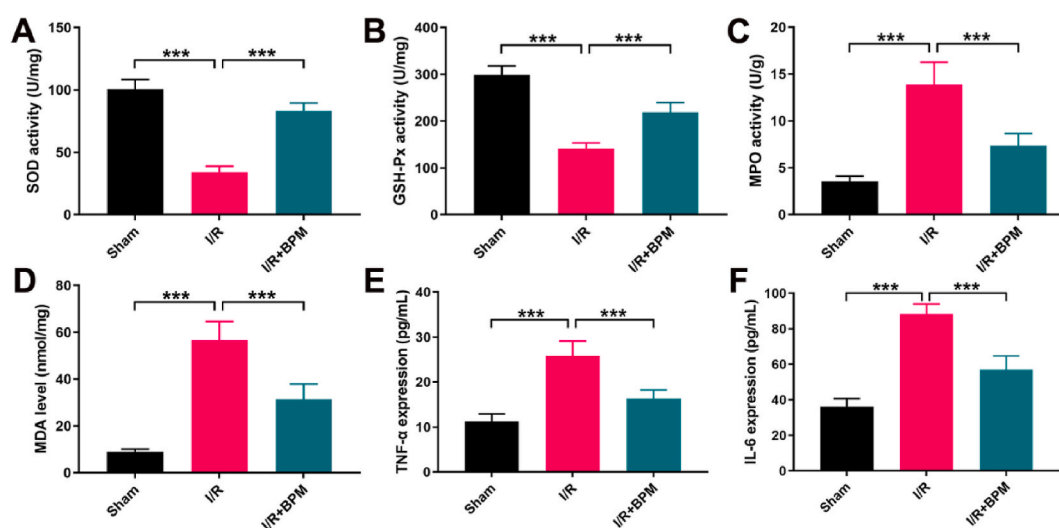
Fig. 2. BPM inhibited oxidative stress and inflammation in I/R-injured flaps. SOD (A), GSH-Px (B), MPO (C), and MDA (D) levels within flap tissue were analyzed through chemical chromatometry. ELISA was also conducted to determine the levels of proinflammatory factors, such as TNF-α (E) and IL-6 (F). The results are presented as the means ± SDs. *P < 0.05, **P < 0.01, and ***P < 0.001; ns, not significant.

and inflammation.

The therapeutic efficacy of BPM in skin flap I/R injury was mediated by the regulation of the Nrf2/HO-1 and TLR4/NF-κB pathways.

Based on our aforementioned results, BPM significantly negatively suppressed oxidative stress and inflammatory responses. To validate the mechanism related to the protective effect of BPM, pathways related to the therapeutic efficacy of BPM were evaluated. Given that NF-κB plays an important role in inflammation, we examined how BPM affects its activation in skin samples. Here, compared with those in the Sham group, the I/R injury group showed marked upregulation of TLR4, *p*-IκB, p-p65, IL-6, and TNF-α (Fig. 3A–G). Nonetheless, the protein levels were apparently downregulated after BPM treatment. Moreover, we examined oxidative stress-related protein levels. Nrf2 and HO-1 levels in the I/R group apparently decreased. Consistently, treatment with BPM was capable of restoring or enhancing Nrf2 and HO-1 levels (Fig. 3H–J). I/R injury elevated Keap1 expression within skin samples, but BPM markedly reduced Keap1 expression (Fig. 3H and K), leading to the activation of Nrf2. Taken together, our data demonstrated that BPM contributed to the protective effects of I/R injury on skin flaps by activating the Nrf2/HO-1 pathway and hindering the TLR4/NF-κB pathway.

3.3. BPM regulated the transcript expression of inflammation and oxidative stress indicators

To determine how BPM affects I/R-injured skin flaps, proinflammatory factor and Nrf2 mRNA expression in skin samples was determined via qRT–PCR. Consistent with the protein levels, I/R injury markedly increased the mRNA expression of proinflammatory factors, such as *TLR4*, *TNF-α*, *IL-6*, and *IL-1β* (Fig. 4A–D). Treatment with BPM almost completely suppressed this upregulation (Fig. 4A–D). Additionally, *Nrf2* and *HO*-1 mRNA expression in the I/R group was dramatically lower than that in the Sham control group (Fig. 4E and F). Again, treatment of rats with BPM significantly antagonized I/R-induced changes (Fig. 4E and F). As revealed by the mRNA regulatory results, BPM had favorable effects on I/R-injured skin flaps by modulating the Nrf2/HO-1 and TLR4/NFκB pathways.

3.4. BPM exerted antioxidant and anti-inflammatory effects by scavenging endogenous ROS in vitro

Low cytotoxicity is an important factor for investigating whether antioxidant and anti-inflammatory agents can be added to cells as free radical scavengers. Therefore, the *in vitro* cytotoxicity of BPM was assessed by observing the cell survival rate after BPM incubation. As shown in Fig. 5A, the non-BPM-treated cells were assigned a 100 % cell viability. BPM exhibited lower cytotoxicity at <200 μg/mL (Fig. 5A). However, when the doses of BPM increased from 200 to 800 μg/mL, the cell viability markedly decreased from 110.4 % to 52.3 %, respectively (Fig. 5A). Therefore, we chose a dose of 200 μg/mL for analyzing inflammation and oxidative stress marker
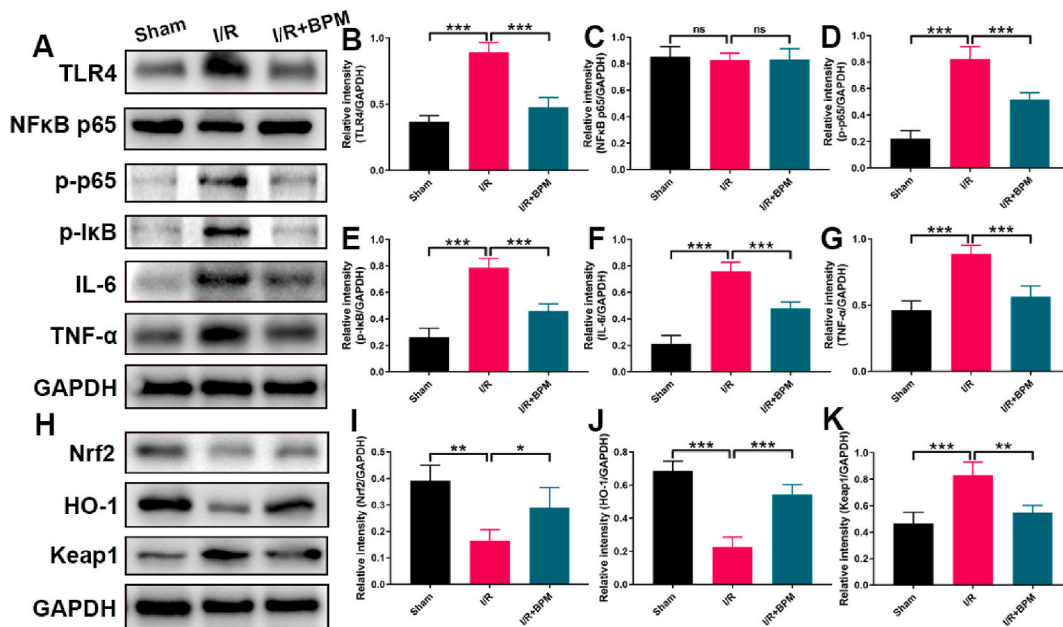

Fig. 3. BPM inhibited the TLR4/NF-κB pathway and enhanced the Nrf2/HO-1 pathway within I/R-injured skin flaps. (A) Western blotting was conducted to determine the protein levels of TLR4, *p*-IκB, NFκB p65, p-p65, IL-6, and TNF-α. (B–G) TLR4, *p*-IκB, NFκB p65, p-p65, IL-6, and TNF-α protein levels were normalized to those of GAPDH. (H) Western blotting was conducted to analyze Nrf2, HO-1, and Keap1 protein expression. (I–K) The graphs indicate the quantitative results. Three separate assays were carried out, and the results were similar. The results are presented as the means ± SDs. *P < 0.05, **P < 0.01, and ***P < 0.001; ns, not significant.
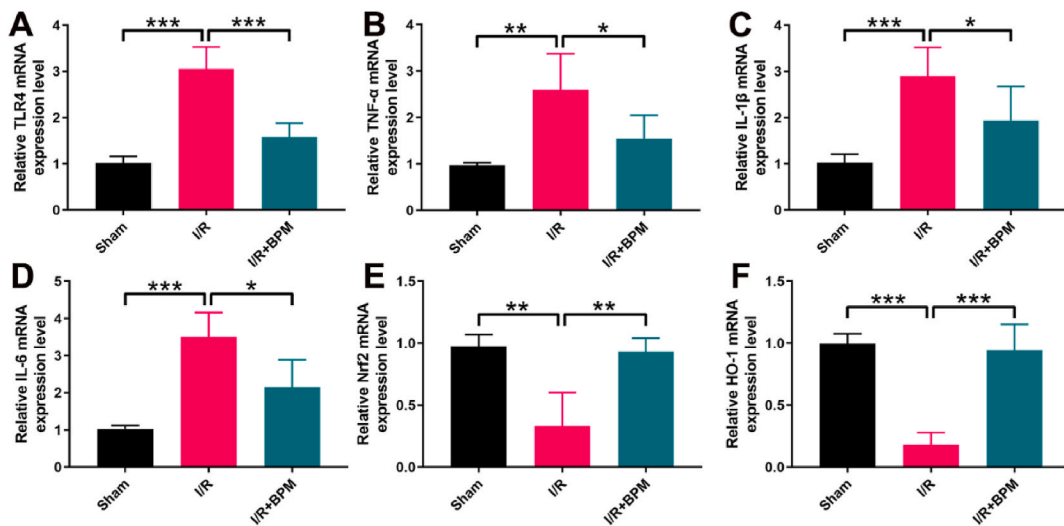
Fig. 4. BPM regulated proinflammatory factors and Nrf2 at the transcript level. The mRNA expression of proinflammatory factors, such as *TLR4* (A), *TNF-α* (B), *IL-1β* (C), and *IL-6* (D), and oxidative stress-associated proteins, such as *Nrf2* (E) and *HO-1* (F), in skin tissues was measured through RT–qPCR, with GAPDH serving as the endogenous reference. The results are presented as the means ± SDs. *P < 0.05, **P < 0.01, and ***P < 0.001; ns, not significant.

protein levels in BMP-treated LPS-triggered RAW 264.7 cells. As demonstrated in Fig. 5B, the scavenging capabilities toward DPPH radicals were significantly enhanced when the treatment of BPM were dose-dependently increased.

Under normal conditions, cells can balance endogenous antioxidase activities precisely to maintain low ROS levels. Therefore, fluorescence images revealed H_2O_2-mediated ROS generation and BPM-induced ROS scavenging in RAW 264.7 cells (Fig. 5C and D). BPM evidently scavenged endogenous ROS relative to H_2O_2-treated cells, as evidenced by the reduced green fluorescence/ROS signal intensity (Fig. 5C and D). In addition, endogenous antioxidases such as SOD and the nonenzymatic antioxidant GSH-Px can prevent the release of cytotoxic ROS and reactive nitrogen species (RNS) in cells and organisms. To determine the mechanism by which BPM scavenges endogenous ROS in H_2O_2-treated RAW 264.7 cells, we measured SOD and GSH-Px antioxidase activities in RAW 264.7 cells (Fig. 5E and F). SOD and GSH-Px activities in RAW 264.7 cells decreased after 100 μmol/L H_2O_2 treatment but were markedly elevated in H_2O_2-treated RAW 264.7 cells following BPM treatment. These findings indicate that BPM could prevent H_2O_2-mediated reductions in SOD and GSH-Px activity within RAW 264.7 cells, likely facilitating antioxidant and anti-inflammatory activities.

BPM ameliorated inflammation and oxidative stress in LPS-stimulated RAW 264.7 cells via activation of Nrf2/HO-1 and suppression of the TLR4/NF-κB pathway in a dose-dependent manner.

To elucidate the critical mechanisms related to the potential function of BPM, we analyzed indicators related to inflammation and oxidative stress in LPS-treated RAW 264.7 cells after treatment with BPM at various doses. As a result, LPS markedly promoted TLR4, p-p65, *p*-IκB, IL-6, TNF-α, and Keap1 expression but reduced Nrf2 and HO-1 expression in RAW 264.7 cells (Fig. 6A and B), suggesting that LPS plays a role in activating inflammation- and oxidative stress-related pathways. BPM administration significantly reversed the changes in the expression of the above proteins in a dose-dependent manner (Fig. 6A–J). Thus, herein we demonstrated that BPM could suppress the upregulation of proinflammatory factors and oxidative stress by activating Nrf2/HO-1 while suppressing the TLR4/NF-κB signaling pathways in a dose-dependent manner.

4. Discussion

Progress is being made in repair and reconstruction surgery, and different free flap graft reconstruction surgeries are being performed in clinical practice [40,41]. Avoiding I/R injury during free flap transplantation can be challenging, and it may cause complete or partial flap necrosis [42,43]. It is important to explore I/R injury mechanisms and discover efficient agents for reducing and preventing skin I/R injury. A number of bioactive peptides, such as collagen from fishes and crude mucus from catfish, may be used to accelerate skin repair [44–46]. Many peptides with low molecular weights can be easily absorbed and may display favorable physiological effects, such as anti-inflammatory, antioxidative, antimicrobial, and skin repair effects, as well as improved collagen synthesis [47–49]. As reported in one prior study, a cecropin-like maggot-derived peptide displayed strong anti-inflammatory and antimicrobial effects on gram-negative bacteria [50]. Our previous works [51,52] verified that maggot extracts protected against acute inflammation and oxidative stress in ulcerative colitis. This study clearly demonstrated that BPM exerted a protective effect on flap I/R injury and promoted flap survival while reducing inflammatory factor levels and oxidative stress injury, and the specific molecular mechanism related to the role of BPM in flap I/R injury might be correlated with the regulation of the Nrf2/HO-1 and TLR4/NF-κB pathways.

To further understand the molecular mechanism related to flap I/R injury, we constructed a flap I/R injury rat model. Eight days after surgery, flap survival rates were determined. The results showed that I/R group had markedly decreased flap survival, whereas I/
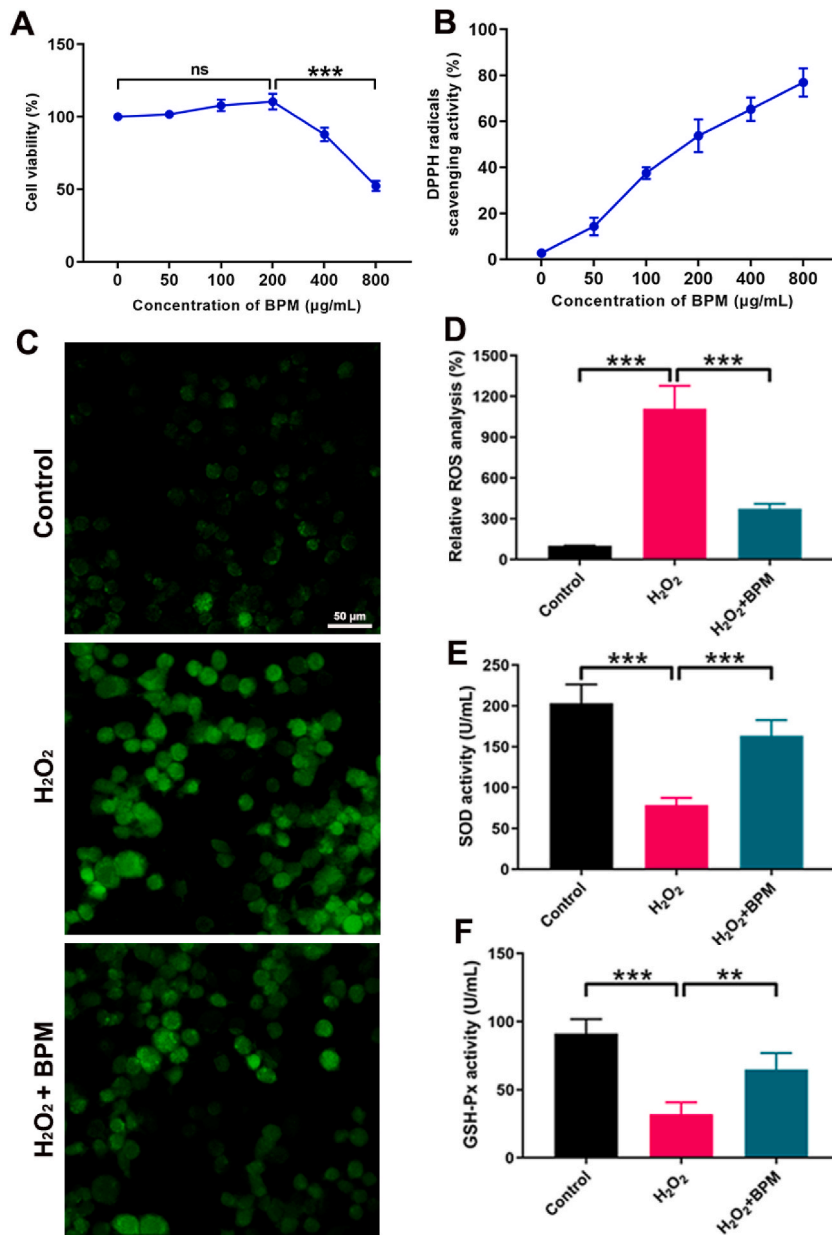
Fig. 5. BPM was capable of scavenging endogenous ROS and increasing antioxidant enzyme activities *in vitro*. (A) RAW 264.7 cell activity following 24-h BPM treatment at various doses (0, 50, 100, 200, 400, and 800 μg/mL). (B) The DPPH radicals scavenging activities of BPM were increased dose-dependently. (C–D) Cells were stimulated with H_2O_2 for a 30-min period, and BMP was added as therapy. Green fluorescence indicates the amount of ROS produced (scale bar: 50 μm). (E–F) SOD and GSH-Px activities in RAW 264.7 cells were analyzed through chemical chromatometry. The results are presented as the means ± SDs. *$P < 0.05$, **$P < 0.01$, and ***$P < 0.001$; ns, not significant.

R + BPM group showed markedly increased flap survival, compared to I/R group, suggesting that BPM could protect I/R injury within the skin flap. The inflammatory response has a critical effect on I/R-injured skin flaps [53]. Inflammatory cytokines can enhance macrophages, causing validated cascades and aggravated tissue injury [54]. As shown in other studies, oxidants, such as ROS and lipid peroxides, are involved in flap graft reconstruction operations, thus leading to I/R injury [55]. Our findings indicated that rats experiencing skin flap I/R presented elevated TNF-α and IL-6 expression, and BPM intake markedly downregulated these proinflammatory factors. In addition, SOD and GSH-Px activities were markedly enhanced, whereas MPO and MDA levels were markedly decreased within skin tissues in the I/R group. Administration of BPM suppressed these alterations. Thus, it was confirmed that BPM regulated I/R injury within the flap skin.

The Nrf2/HO-1 and TLR4/NF-κB pathways play important roles in the inflammatory response and oxidative stress during I/R injury. The Nrf2 pathway regulates numerous antioxidant proteins and detoxification enzymes, such as GSH-Px, HO-1, and SOD.
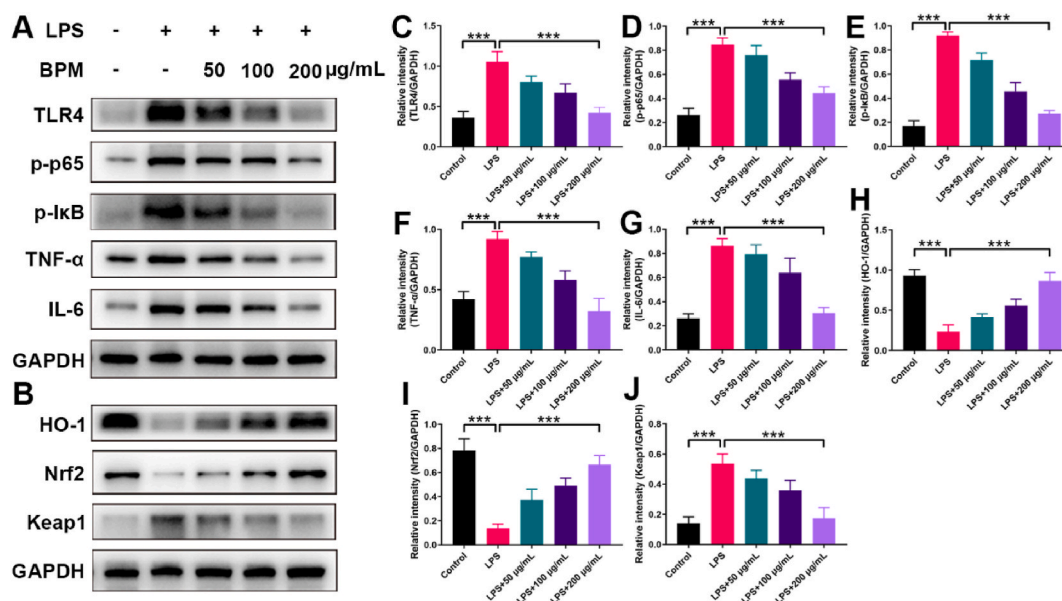
Fig. 6. BPM dose-dependently suppressed inflammation and oxidative stress in LPS-stimulated RAW 264.7 cells. (A–B) TLR4, *p*-IκB, p-p65, IL-6, TNF-α, Nrf2, HO-1, and Keap1 protein levels were determined through Western blotting. (C–J) The graphs indicate the quantitative results. Three separate assays were conducted to obtain the results. The results are presented as the means ± SDs. *P < 0.05, **P < 0.01, and ***P < 0.001; ns, not significant.

Consequently, the Nrf2 pathway has a critical effect on the cellular defense system [38]. Activated Nrf2, which positively regulates HO-1 transcription, has an important effect on decreasing gastrointestinal inflammation together with oxidative stress [56,57]. The redox-sensitive transcription factor NFκB plays a crucial role in innate immunity, inflammation, and tissue integrity maintenance and can modulate the levels of proinflammatory cytokines, such as TLR4, p-p65, *p*-IκB, IL6, and TNF-α, eventually inducing immune dysfunction and local inflammation and triggering the positive feedback loop that induces inflammation, causing I/R injury [58,59]. As reported in other studies, erythropoietin pretreatment mitigates lung I/R injury through the TLR4/NF-κB pathway [60]. In addition, recombinant human growth hormone and luteolin protect against skin flap I/R injury through the TLR4/NF-κB pathway and decrease ROS levels [61]. According to our data, BPM exerted direct suppressive effects on the upregulation of proinflammatory cytokines, including TLR4, *p*-IκB, p-p65, TNF-α, and IL-6. Additionally, following BPM treatment, it directly activated Nrf2 and HO-1 in I/R injury. Consistently, the anti-inflammatory and antioxidative functions of BPM were confirmed *in vitro*. According to the results of the CCK-8 assay, 24 h of BPM treatment at 200 μg/mL did not obviously change RAW 264.7 cell viability, suggesting that BPM had a mild cytotoxic effect. The excellent efficacy and low toxicity of BPM *in vivo* highlighted that BPM might be useful for treating skin flap I/R injury.

To conclude, our findings demonstrated that BPM has therapeutic efficacy on I/R-injured skin flaps. This work is the first to clarify that the mechanisms underlying BPM are possibly associated with the inhibition of the inflammatory response and oxidative stress damage by Nrf2/HO-1, as well as the TLR4/NF-κB pathway. Based on the above findings, BPM may serve as a promising compound for the therapy of flap I/R injury.

Ethics approval and consent to participate

Consent for publication

Not applicable.

Data availability statement

The data will be made available upon request.

CRediT authorship contribution statement

Hao Chen: Writing – review & editing, Conceptualization. **Tianqi Zhang:** Formal analysis, Data curation. **Su Yan:** Project administration, Methodology. **Shan Zhang:** Software, Resources. **Qiuyue Fu:** Validation, Supervision. **Chuchu Xiong:** Visualization, Validation. **Lina Zhou:** Investigation, Formal analysis. **Xiao Ma:** Methodology, Investigation, Formal analysis. **Rong Wang:** Writing – review & editing, Writing – original draft, Visualization, Data curation, Conceptualization. **Gang Chen:** Writing – original draft, Visualization, Supervision.

Declaration of competing interest

The authors declare that they have no known competing financial interests or personal relationships that could have appeared to influence the work reported in this paper.

Appendix A. Supplementary data

Supplementary data to this article can be found online at https://doi.org/10.1016/j.heliyon.2024.e29874.

References

[1] B.T. Varghese, P. Vijayakumar, R.R. Ani, S. Thomas, Salvaging skin loss of free fibular osteo-cutaneous flaps in oral oncological reconstruction, Oral Oncol. 97 (2019) 131–132.

[2] D. Wendling, M. Guidet, Osteolytic Paget's disease of bone under unduly etidronate therapy, Clin. Rheumatol. 7 (1988) 543–545.

[3] B. Liu, Q. Xu, J. Wang, et al., Recombinant human growth hormone treatment of mice suppresses inflammation and apoptosis caused by skin flap ischemia-reperfusion injury, J. Cell. Biochem. 120 (2019) 18162–18171.

[4] T. Hao, M. Qian, Y. Zhang, et al., An injectable dual-function hydrogel protects against myocardial ischemia/reperfusion injury by modulating ROS/NO disequilibrium, Adv. Sci. 9 (2022) e2105408.

[5] L. Jiang, X. Yin, Y.H. Chen, et al., Proteomic analysis reveals ginsenoside Rb1 attenuates myocardial ischemia/reperfusion injury through inhibiting ROS production from mitochondrial complex I, Theranostics 11 (2021) 1703–1720.

[6] Z. Zhao, J. Wu, H. Xu, et al., XJB-5-131 inhibited ferroptosis in tubular epithelial cells after ischemia-reperfusion injury, Cell Death Dis. 11 (2020) 629.

[7] J. Ju, R. Hou, P. Zhang, D-allose alleviates ischemia/reperfusion (I/R) injury in skin flap via MKP-1, Mol. Med. 26 (2020) 21.

[8] Y.Q. Jiang, X.Y. Yang, D.Q. Duan, et al., Inhibition of MALT1 reduces ferroptosis in rat hearts following ischemia/reperfusion via enhancing the Nrf2/SLC7A11 pathway, Eur. J. Pharmacol. 950 (2023) 175774.

[9] U. Acaroz, S. Ince, D. Arslan-Acaroz, et al., Bisphenol-A induced oxidative stress, inflammatory gene expression, and metabolic and histopathological changes in male Wistar albino rats: protective role of boron, Toxicol res-uk 8 (2019) 262–269.

[10] N. Ramazani, G.F. Mahd, A. Soleimanzadeh, et al., The influence of L-proline and fulvic acid on oxidative stress and semen quality of buffalo bull semen following cryopreservation, Vet. Med. Sci. 9 (2023) 1791–1802.

[11] M.G. van den Heuvel, A. Bast, G.R. Haenen, A.W. Ambergen, J.F. Mermans, R.R. van der Hulst, The role of antioxidants in ischaemia-reperfusion in a human DIEP flap model, J Plast Reconstr Aes 65 (2012) 1706–1711.

[12] C.X. Shi, Y.B. Ding, F. Jin, et al., Effects of sevoflurane post-conditioning in cerebral ischemia-reperfusion injury via TLR4/NF-kappaB pathway in rats, Eur Rev Med Pharmaco 22 (2018) 1770–1775.

[13] X. Zhao, S. Li, Y. Mo, et al., DCA protects against oxidation injury attributed to cerebral ischemia-reperfusion by regulating glycolysis through PDK2-PDH-nrf2 Axis, Oxid. Med. Cell. Longev. 2021 (2021) 5173035.

[14] D.M. Losada, M.E. Jordani, M.C. Jordani, et al., Should preconditioning hyperbaric oxygenation protect the liver against ischemia-reperfusion injury? An experimental study in a rat model, Transpl P 46 (2014) 56–62.

[15] D.J. Hausenloy, D.M. Yellon, Ischaemic conditioning and reperfusion injury, Nat. Rev. Cardiol. 13 (2016) 193–209.

[16] J.G. Wright, J.C. Kerr, C.R. Valeri, R.N. Hobson, Heparin decreases ischemia-reperfusion injury in isolated canine gracilis model, Arch. Surg. 123 (1988) 470–472.

[17] A. Gurlek, M. Celik, H. Parlakpinar, H. Aydogan, A. Bay-Karabulut, The protective effect of melatonin on ischemia-reperfusion injury in the groin (inferior epigastric) flap model in rats, J. Pineal Res. 40 (2006) 312–317.

[18] K.Y. Polat, B. Aydinli, O. Polat, et al., The protective effect of aprotinin and alpha-tocopherol on ischemia-reperfusion injury of the rat liver, TRANSPL P 40 (2008) 63–68.

[19] R. Wang, Y. Luo, Y. Lu, et al., Maggot extracts alleviate inflammation and oxidative stress in acute experimental colitis via the activation of Nrf2, Oxid. Med. Cell. Longev. 2019 (2019) 4703253.

[20] H. Ai, F. Wang, N. Zhang, L. Zhang, C. Lei, Antiviral, immunomodulatory, and free radical scavenging activities of a protein-enriched fraction from the larvae of the housefly, Musca domestica, J. Insect Sci. 13 (2013) 112.

[21] W. Wang, M. Zhong, T. Yu, et al., Polysaccharide extracted from WuGuChong reduces high-fat diet-induced obesity in mice by regulating the composition of intestinal microbiota, Nutr. Metab. 17 (2020) 27.

[22] P.N. Li, H. Li, L.X. Zhong, et al., Molecular events underlying maggot extract promoted rat in vivo and human in vitro skin wound healing, Wound Repair Regen. 23 (2015) 65–73.

[23] H. Alipour, M. Shahriari-Namadi, S. Ebrahimi, M.D. Moemenbellah-Fard, Wound healing potential: evaluation of molecular profiling and amplification of Lucilia sericata angiopoietin-1 mRNA mid-part, BMC Res. Notes 13 (2020) 308.

[24] Z.M. Mohd, S. Holloway, N.N. Mohd, Maggot therapy in wound healing: a systematic review, Int. J. Environ. Res. Publ. Health 17 (2020).

[25] G. Shamloul, A. Khachemoune, Reappraisal and updated review of maggot debridement therapy in chronic lower extremity ulcers, Int. J. Dermatol. 62 (2023) 962–968.

[26] H. Mei, J. Xu, Y. He, et al., Protein-rich extract of Musca domestica larvae alleviated metabolic disorder in STZ-induced type 2 diabetic rat model via hepatoprotective and pancreatic beta-cell protective activities, J Biosciences 43 (2018) 969–983.

[27] Z. Zhang, S. Wang, Y. Diao, J. Zhang, D. Lv, Fatty acid extracts from Lucilia sericata larvae promote murine cutaneous wound healing by angiogenic activity, Lipids Health Dis. 9 (2010) 24.

[28] S. Staczek, M. Cytrynska, A. Zdybicka-Barabas, Unraveling the role of antimicrobial peptides in insects, Int. J. Mol. Sci. 24 (2023).

[29] J. Yun, J.S. Hwang, D.G. Lee, The antifungal activity of the peptide, periplanetasin-2, derived from American cockroach Periplaneta americana, Biochem. J. 474 (2017) 3027–3043.

[30] M.E. Borges, R.L. Tejera, L. Diaz, P. Esparza, E. Ibanez, Natural dyes extraction from cochineal (Dactylopius coccus). New extraction methods, Food Chem. 132 (2012) 1855–1860.

[31] F.G. Hall, O.G. Jones, M.E. O'Haire, A.M. Liceaga, Functional properties of tropical banded cricket (Gryllodes sigillatus) protein hydrolysates, Food Chem. 224 (2017) 414–422.

[32] H. Chen, Z. Xu, F. Fan, et al., Identification and mechanism evaluation of a novel osteogenesis promoting peptide from Tubulin Alpha-1C chain in Crassostrea gigas, Food Chem. 272 (2019) 751–757.

[33] G. Feng, J. Wu, H.L. Yang, L. Mu, Discovery of antioxidant peptides from Amphibians: a review, Protein Peptide Lett 28 (2021) 1220–1229.

[34] P. Shi, T. Zhao, W. Wang, et al., Protective effect of homogeneous polysaccharides of Wuguchong (HPW) on intestinal mucositis induced by 5-fluorouracil in mice, Nutr. Metab. 19 (2022) 36.

[35] Y. Li, H. Liu, Z. Zeng, et al., Ginsenoside Rb3 attenuates skin flap ischemia-reperfusion damage by inhibiting STING-IRF3 signaling, J. Mol. Histol. 53 (2022) 763–772.

[36] N. Otani, K. Tomita, Y. Kobayashi, et al., Hydrogen-generating Si-based agent protects against skin flap ischemia-reperfusion injury in rats, Sci Rep-Uk 12 (2022) 6168.

[37] Z. Yin, H. Ren, L. Liu, et al., Thioredoxin protects skin flaps from ischemia-reperfusion injury: a novel prognostic and therapeutic target, Plast. Reconstr. Surg. 137 (2016) 511–521.

[38] R. Wang, L. Zheng, Q. Xu, et al., Unveiling the structural properties of water-soluble lignin from gramineous biomass by autohydrolysis and its functionality as a bioactivator (anti-inflammatory and antioxidative), Int. J. Biol. Macromol. 191 (2021) 1087–1095.

[39] W. Pei, Z.S. Chen, H. Chan, L. Zheng, C. Liang, C. Huang, Isolation and identification of a novel anti-protein aggregation activity of lignin-carbohydrate complex from chionanthus retusus leaves, Front Bioeng Biotech 8 (2020) 573991.

[40] R.N. Ciofu, D.G. Zamfirescu, S.A. Popescu, I. Lascar, Reverse sural flap for ankle and heel soft tissues reconstruction, J Med Life 10 (2017) 94–98.

[41] S. Hernot, R. Wadhera, M. Kaintura, et al., Tracheocutaneous fistula closure: comparison of rhomboid flap repair with Z plasty repair in a case series of 40 patients, Aesthet Plast Surg 40 (2016) 908–913.

[42] N. Nemeth, I. Furka, I. Miko, Hemorheological changes in ischemia-reperfusion: an overview on our experimental surgical data, Clin Hemorheol Micro 57 (2014) 215–225.

[43] G. Zhao, X. Zhang, P. Xu, J.Y. Mi, Y.J. Rui, The protective effect of Irisin against ischemia-reperfusion injury after perforator flap grafting in rats, Injury 49 (2018) 2147–2153.

[44] S. Bragadeeswaran, S. Priyadharshini, K. Prabhu, S.R. Rani, Antimicrobial and hemolytic activity of fish epidermal mucus Cynoglossus arel and Arius caelatus, Asian Pac. J. Tropical Med. 4 (2011) 305–309.

[45] S. Veeraperumal, H.M. Qiu, S.S. Zeng, et al., Polysaccharides from Gracilaria lemaneiformis promote the HaCaT keratinocytes wound healing by polarised and directional cell migration, Carbohyd Polym 241 (2020) 116310.

[46] F. Yang, S. Jin, Y. Tang, Marine collagen peptides promote cell proliferation of NIH-3T3 fibroblasts via NF-kappaB signaling pathway, Molecules 24 (2019).

[47] R. Hartmann, H. Meisel, Food-derived peptides with biological activity: from research to food applications, Curr. Opin. Biotechnol. 18 (2007) 163–169.

[48] L.X. He, Z.F. Zhang, B. Sun, et al., Sea cucumber (Codonopsis pilosula) oligopeptides: immunomodulatory effects based on stimulating Th cells, cytokine secretion and antibody production, Food Funct. 7 (2016) 1208–1216.

[49] Z. Hu, P. Yang, C. Zhou, S. Li, P. Hong, Marine collagen peptides from the skin of nile Tilapia (Oreochromis niloticus): characterization and wound healing evaluation, Mar. Drugs 15 (2017).

[50] G.A. Tellez, J.A. Zapata, L.J. Toro, et al., Identification, characterization, immunolocalization, and biological activity of lucilin peptide, Acta Trop. 185 (2018) 318–326.

[51] R. Wang, D. Wang, H. Wang, et al., Therapeutic targeting of Nrf2 signaling by maggot extracts ameliorates inflammation-associated intestinal fibrosis in chronic DSS-induced colitis, Front. Immunol. 12 (2021) 670159.

[52] R. Wang, L. Wang, Y. Luo, et al., Maggot protein ameliorates dextran sulphate sodium-induced ulcerative colitis in mice, Bioscience Rep 38 (2018).

[53] Y.C. Chang, W.J. Xue, W. Ji, et al., The protective effect of propofol against ischemia-reperfusion injury in the interlobar arteries: reduction of abnormal Cx43 expression as a possible mechanism, Kidney Blood Press R 43 (2018) 1607–1622.

[54] E.M. Muntjewerff, G. Dunkel, M. Nicolasen, S.K. Mahata, G. van den Bogaart, Catestatin as a target for treatment of inflammatory diseases, Front. Immunol. 9 (2018) 2199.

[55] T. Kuroki, S. Takekoshi, C. Kitatani, C. Kato, M. Miyasaka, T. Akamatsu, Protective effect of ebselen on ischemia-reperfusion injury in epigastric skin flaps in rats, Acta Histochem. Cytoc. 55 (2022) 149–157.

[56] Z. Kohandel, T. Farkhondeh, M. Aschner, A.M. Pourbagher-Shahri, S. Samarghandian, Anti-inflammatory action of astaxanthin and its use in the treatment of various diseases, Biomed. Pharmacother. 145 (2022) 112179.

[57] J. Chen, J. Zhang, T. Chen, et al., Xiaojianzhong decoction attenuates gastric mucosal injury by activating the p62/Keap1/Nrf2 signaling pathway to inhibit ferroptosis, Biomed. Pharmacother. 155 (2022) 113631.

[58] W. Liang, C. Lin, L. Yuan, et al., Preactivation of Notch1 in remote ischemic preconditioning reduces cerebral ischemia-reperfusion injury through crosstalk with the NF-kappaB pathway, J Neuroinflamm 16 (2019) 181.

[59] Z. Xu, X. Sun, B. Ding, M. Zi, Y. Ma, Oleuropein ameliorated lung ischemia-reperfusion injury by inhibiting TLR4 signaling cascade in alveolar macrophages, Transpl. Immunol. 74 (2022) 101664.

[60] Q. He, X. Zhao, S. Bi, Y. Cao, Pretreatment with erythropoietin attenuates lung ischemia/reperfusion injury via toll-like receptor-4/nuclear factor-kappaB (TLR4/NF-kappaB) pathway, Med Sci Monitor 24 (2018) 1251–1257.

[61] G. Chen, H. Shen, L. Zang, et al., Protective effect of luteolin on skin ischemia-reperfusion injury through an AKT-dependent mechanism, Int. J. Mol. Med. 42 (2018) 3073–3082.